Isolation and Crystallographic Characterization of the Labile Isomer of Y@C82 Cocrystallized with Ni(OEP): Unprecedented Dimerization of Pristine Metallofullerenes

Lipiao Bao, Changwang Pan, Zdenek Slanina, Filip Uhlik, Takeshi Akasaka, and Xing Lu*

Dedicated to Professor Zhennan Gu on the occasion of his 80th birthday

Abstract: Although the major isomers of $M@C_{82}$ (namely $M@C_{2v}(9)$-C_{82}, where M is a trivalent rare-earth metal) have been intensively investigated, the lability of the minor isomers has meant that they have been little studied. Herein, the first isolation and crystallographic characterization of the minor $Y@C_{82}$ isomer, unambiguously assigned as $Y@C_s(6)$-C_{82} by cocrystallization with Ni(octaethylporphyrin), is reported. Unexpectedly, a regioselective dimerization is observed in the crystalline state of $Y@C_s(6)$-C_{82}. In sharp contrast, no dimerization occurs for the major isomer $Y@C_{2v}(9)$-C_{82} under the same conditions, indicating a cage-symmetry-induced dimerization process. Further experimental and theoretical results disclose that the regioselective dimer formation is a consequence of the localization of high spin density on a special cage-carbon atom of $Y@C_s(6)$-C_{82} which is caused by the steady displacement of the Y atom inside the $C_s(6)$-C_{82} cage.

$\mathbf{A}$lthough C_{60} and C_{70} are the most abundant empty fullerenes, the larger fullerene cage C_{82} is unique for endohedral metallofullerene (EMF), that is, a fullerene molecule with metal atom(s) or metallic cluster(s) inside.[1,2] As early as 1991, the Smalley and co-workers reported the first solvent extraction of the prototypical La@C82,[3] opening the door to studying the solution chemistry of EMFs. Theoretical studies indicated that the $C_{2v}(9)$-C_{82} isomer is more stable for La@C82, followed by $C_{3v}(8)$-C_{82} and $C_s(6)$-C_{82}, by assuming that three electrons are transferred from the internal La atom to the cage.[4] Two isomers have been isolated for La@C82 and their molecular structures were later

determined by Akasaka and co-workers by using NMR measurements.[5,6] The assignment of the structure of the major isomer as La@$C_{2v}(9)$-C_{82} was straightforward because the observed $[17 \times 4 + 7 \times 2]$ pattern is in perfect agreement with the $C_{2v}(9)$-C_{82} cage if only isomers obeying the isolated pentagon rule (IPR) are considered. However, the $[38 \times 2 + 6 \times 1]$ NMR pattern of the minor La@C82 isomer can be assigned to any of the three IPR C_s-symmetric C_{82} cages and theoretical results suggested that La@$C_s(6)$-C_{82} should be the most stable one. Since theoretical predictions are not always convincing even for monometallic EMFs (for example, La@$C_{3v}(7)$-C_{82} was experimentally obtained although the theoretical results suggested that La@$C_{3v}(8)$-C_{82} is more stable),[7] the structure of the minor La@C82 isomer is still not truly clear because of the lack of unambiguous single-crystal X-ray crystallographic results, especially concerning the position of the metal center.

Another important compound based on a C_{82} cage is Y@C82. In 1995, Takata and co-workers performed synchrotron X-ray studies on a powder of Y@C82 to confirm the endohedral nature of EMFs for the first time.[8] However, it is still not clear whether the sample contained a pure Y@C82 isomer or if it was a mixture of two or more regioisomers. In fact, previous EPR studies indicated that the main signals for the extraction of Y-based EMFs can be ascribed to a major Y@C82 isomer, but some unresolved EPR signals were difficult to assign.[9–12] It was once assumed that these additional EPR signals were attributable to $Y_2@C_{82}$ in a triplet ground state[12] or that they originated from the hyperfine coupling of the yttrium atom to ^{13}C on the C_{82} cage.[10] By supposing the existence of another Y@C82 isomer, the complicated EPR spectrum of Y-based EMFs could be well reproduced.[11] Hoinkis and co-workers proposed that the two Y@C82 isomers may differ in either the metal position or the cage symmetry, in addition to uncharacterized adducts, solvent molecules, or hollow fullerenes which could also contribute to these additional EPR signals.[9] In an effort to isolate Y@C82 isomers, the minor Y@C82 isomer disappeared after the HPLC separation as a result of decomposition, although it was detected along with the major Y@C82 isomer by EPR spectroscopy.[13] Accordingly, this long-sought isomer is viewed as a "ghost" compound with no information about its structure and properties available to date.[9–13] In sharp contrast, NMR spectroscopic results proposed that the major Y@C82 isomer has the $C_{2v}(9)$-C_{82} cage and X-ray results of its

[*] L. Bao, C. Pan, Prof. T. Akasaka, Prof. X. Lu
State Key Laboratory of Materials Processing and Die & Mold Technology, School of Materials Science and Engineering
Huazhong University of Science and Technology
1037, Luoyu Road, Wuhan 430074 (P.R. China)
E-mail: lux@hust.edu.cn

Prof. Z. Slanina
Life Science Center of Tsukuba Advanced Research Alliance
University of Tsukuba
Tsukuba, Ibaraki 305-8577 (Japan)

Prof. F. Uhlik
Department of Physical and Macromolecular Chemistry
Charles University in Prague
12843 Prague 2 (Czech Republic)

Supporting information and the ORCID identification number(s) for the author(s) of this article can be found under http://dx.doi.org/10.1002/anie.201604121.

carbene derivative firmly confirmed the cage connectivity and the metal location.[14,15]

Herein, we report the synthesis, isolation, and crystallographic characterization of the two isomers of $Y@C_{82}$. These results reveal unambiguously the molecular structures of the two isomers as $Y@C_{2v}(9)-C_{82}$ and $Y@C_s(6)-C_{82}$, respectively, presenting the first crystallographic results for both isomers with an unfunctionalized cage. Interestingly and unexpectedly, a highly regioselective dimerization occurs for $Y@C_s(6)-C_{82}$ in the crystalline state, which has not been previously reported for any pristine EMFs. In contrast, $Y@C_{2v}(9)-C_{82}$ does not form dimers under identical crystallization conditions. Theoretical results present a reasonable explanation for this difference by considering the anisotropic distribution of the spin density on the cages, which is induced by the cage geometry as well as the location of the metal center.

Soot containing yttrium EMFs was synthesized by an arc-discharging method[16] and was extracted using *N,N*-dimethylformamide. Subsequent separation by using HPLC gave pure samples of both $Y@C_{82}$ isomers (see the Supporting Information for details). Their vis/NIR absorption spectra are shown in Figure 1. The major $Y@C_{82}$ isomer shows characteristic bands at $\lambda = 640$, 723, 997, and 1405 nm.[13] The spectrum of the minor $Y@C_{82}$ isomer has two absorption bands at $\lambda = 729$ and 1108 nm, which is similar to those of La@C_{82}-II[6] and Pr@C_{82}-II.[17] Since only NMR results were reported for La@C_{82}-II,[6] which cannot unambiguously assign the cage structure and the metal position, single-crystal X-ray results are very desirable.
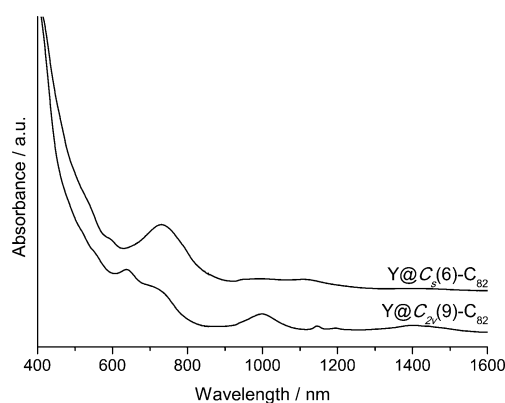

Figure 1. Vis/NIR absorption spectra of $Y@C_s(6)-C_{82}$ and $Y@C_{2v}(9)-C_{82}$ in CS_2 at room temperature. The two curves are vertically shifted for ease of comparison.

Fortunately, we were able to obtain single crystals of both $Y@C_{82}$ isomers which were used to unambiguously determine their molecular structures.[18,19] Both isomers crystallized in the commonly encountered space group $C2/m$, in which one half of the Ni(OEP) molecule (OEP is the dianion of octaethylporphyrin) and two halves of the C_{82} cage are present in the asymmetric unit. However, the crystallographic mirror plane does not coincide with any of the symmetry elements of the C_{82} cages. Accordingly, two cage orientations are present in the system with an equal occupancy of 0.50.

Figure 2 shows the molecular structure of the minor $Y@C_{82}$ isomer, where the fullerene cage is firmly assigned to be $C_s(6)-C_{82}$. Luckily, the internal Y atom resides on the crystallographic mirror plane and thus shows no disorder. As a result, the relative position of the Y atom to either cage orientation is identical. The Y atom is located under a [6,6]-bond (C33−C34) but departs slightly from the mirror plane of the cage. The closest yttrium···cage distances are 2.274 Å for Y···C33 and 2.333 Å for Y···C34. The fixed metal location found for the trivalent Y^{3+} ion here is totally different from the reported situation of the metal centers in $M^{2+}@[C_s(6)-C_{82}]^{2-}$ (M = Yb, Sm),[20,21] where the divalent metal ion shows multiple disordered sites inside the same $C_s(6)-C_{82}$ cage. It thus seems that the ionic state makes the metal ion interact differently with the cage carbon atoms influencing its location and/or motion.

Astonishingly, the crystal structure shows that two $Y@C_s-(6)-C_{82}$ molecules are connected with a C−C single bond of 1.611(2) Å to form a dimeric structure (Figure 2). To the best of our knowledge, this is the first time that the formation of a dimer in the crystal form between two pristine EMF molecules has been reported. Previous studies have merely demonstrated that chemical functionalization of EMFs can alter their electronic configurations, and several special derivatives can form dimers in the crystalline state.[22–24] In addition, the dimerization of $Y@C_s(6)-C_{82}$ occurs in a highly
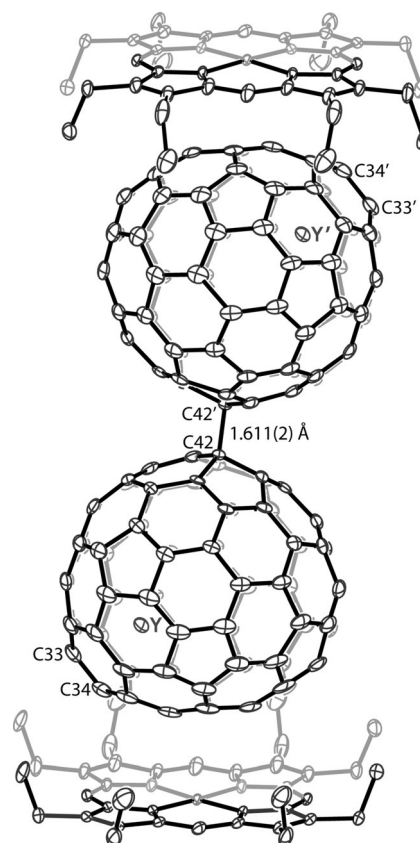

Figure 2. An ORTEP drawing of $[Y@C_s(6)-C_{82}]_2 \cdot 2[Ni(OEP)]$. Thermal ellipsoids are set at 30% probability. Only one cage orientation is shown. Solvent molecules and hydrogen atoms are omitted for clarity.

regioselective fashion at a specific cage carbon atom (C42) which is quite remote from the internal Y atom.

In contrast, the major isomer of Y@C$_{82}$ does not show a dimeric structure under identical crystallization conditions. Figure 3 depicts the molecular structure of the major Y@C$_{82}$ isomer where the cage connectivity is unambiguously assigned as $C_{2v}(9)$-C$_{82}$, consistent with previous crystallographic results of its carbene derivative.[15] Insides the cage, the Y atom shows six disordered positions with fractional occupancy values of 0.195 (Y1), 0.195 (Y1A), 0.110 (Y2), 0.110 (Y2A), 0.220 (Y3), and 0.170 (Y4), respectively, indicating a moving metal atom inside the cage. The major Y disorder site (Y3) resides at an off-center position adjacent to a hexagonal ring. The closest Y⋯cage distance (2.186 Å) in Y@$C_{2v}(9)$-C$_{82}$ is a bit shorter than that (2.274 Å) in Y@$C_s(6)$-C$_{82}$, which should be a consequence of their different cage shapes.
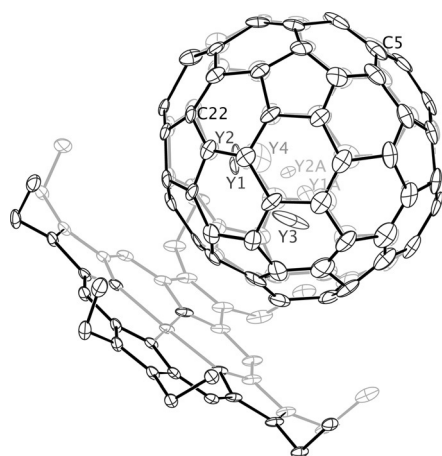

Figure 4. Packing structures of a) [Y@$C_s(6)$-C$_{82}$]$_2$·2[Ni(OEP)]·3(C$_6$H$_6$)·2-(CS$_2$) and b) 2[Y@$C_{2v}(9)$-C$_{82}$]·2[Ni(OEP)]·3(C$_6$H$_6$)·2(CS$_2$). Only one cage orientation is shown for each system. Minor metal sites and solvent molecules are omitted for clarity.

Figure 3. An ORTEP drawing of [Y@$C_{2v}(9)$-C$_{82}$]·[Ni(OEP)]. Thermal ellipsoids are set at 10% probability. Only one cage orientation is shown. Solvent molecules and hydrogen atoms are omitted for clarity.

Figure 5. Spin density distribution of cage carbon atoms of Y@$C_{2v}(9)$-C$_{82}$ and Y@$C_s(6)$-C$_{82}$. The numbering schemes for the carbon atoms are shown in Figure S6. Data is obtained from the optimized structures of monomeric Y@$C_{2v}(9)$-C$_{82}$·Ni(OEP) and Y@$C_s(6)$-C$_{82}$·Ni(OEP).

Both Y@C$_{82}$ isomers adopt similar packing structures in the crystalline state (Figure S5). Figure 4 shows a comparison of their packing structures cocrystallized with Ni(OEP). In contrast to the dimeric situation of Y@$C_s(6)$-C$_{82}$ where the intercage distance is 1.611(2) Å, two adjacent cages of Y@$C_{2v}(9)$-C$_{82}$ are separated by 3.432 Å (C5⋯C5′), confirming that no dimerization occurs. As a consequence, the distance between the Ni(OEP) bilayers in the case of Y@$C_{2v}(9)$-C$_{82}$ (24.142 Å) is significantly longer than that of Y@$C_s(6)$-C$_{82}$ (23.661 Å), despite the fact that the shortest Ni⋯cage distance in Y@$C_{2v}(9)$-C$_{82}$·Ni(OEP) (2.784 Å) is even shorter than that in Y@$C_s(6)$-C$_{82}$·Ni(OEP) (2.848 Å) and the size of Y@$C_{2v}(9)$-C$_{82}$ (7.885 Å) is also smaller than that of Y@$C_s(6)$-C$_{82}$ (8.265 Å).

It is commonly accepted that three electrons are transferred from the internal yttrium atom to the C$_{82}$ cage in Y@C$_{82}$, resulting in an unpaired electron delocalized on the fullerene cage. Accordingly, theoretical calculations were conducted to understand the unexpected dimerization of Y@$C_s(6)$-C$_{82}$ by considering the spin density distribution on th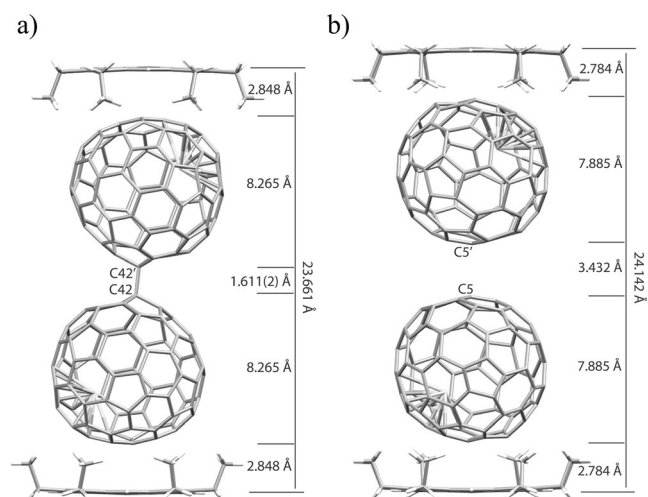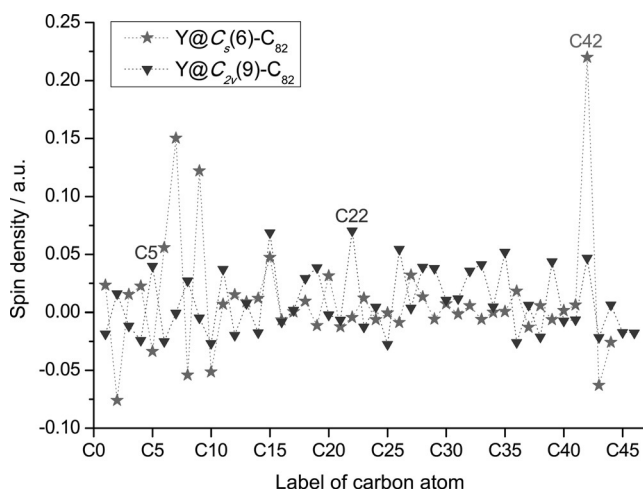e cage. Figure 5 shows the spin density values of the carbon atoms in both Y@C$_{82}$ isomers. Remarkably, some cage carbon atoms of Y@$C_s(6)$-C$_{82}$ bear obvious higher spin density values than other cage carbons regardless of the existence of Ni(OEP) molecules (Figure S7). In particular, the carbon atom at the site of dimerization (C42) has an extremely high spin density value (0.22), and accordingly the C42 atom on two cages tend to connect with each other through a radical coupling reaction in the crystal. In contrast, the spin densities are more evenly distributed on the cage of Y@$C_{2v}(9)$-C$_{82}$. The highest value is found for C22 (0.07), which is more than three times smaller than that in Y@$C_s(6)$-C$_{82}$ (C42: spin density 0.22). As a consequence, the cage carbon atoms of Y@$C_{2v}(9)$-C$_{82}$ do not have high radical characters and do not tend to form dimers. Further calculations reveal that the dimeric structure of Y@$C_s(6)$-C$_{82}$·Ni(OEP) is 51.01 kcal mol^{-1} more

stable than the two monomers, indicating a thermodynamically favorable dimerization process. Obviously, the different distributions of spin densities of both isomers should be a result of their different cage structures which eventually govern the dimerization process of $Y@C_s(6)\text{-}C_{82}$. Such a high radical character of $Y@C_s(6)\text{-}C_{82}$ (particularly C42) makes it highly reactive toward radical species in soot and thus it has never been isolated, a case similar to the insoluble $La@C_{2n}$ ($2n = 72,74,80,82$).[7,25–28] However, the ready solubility of $Y@C_s(6)\text{-}C_{82}$ provides opportunities to study the intrinsic properties of these highly reactive EMFs. It is anticipated that $Y@C_s(6)\text{-}C_{82}$ will show different chemical properties from those of conventional EMFs because of its high radical character.

Cyclic voltammetry (CV) and differential pulse voltammetry (DPV) reveal that $Y@C_s(6)\text{-}C_{82}$ exhibits one reversible oxidation step and three reversible reduction processes (Figure S8). Table 1 presents the redox potentials of both $Y@C_{82}$ isomers. When compared to the corresponding values of $Y@C_{2v}(9)\text{-}C_{82}$, the first reduction potential of $Y@C_s(6)\text{-}C_{82}$ is negatively shifted by 0.09 V but the first oxidation potential is shifted cathodically by 0.17 V. Accordingly, $Y@C_s(6)\text{-}C_{82}$ has an even smaller electrochemical gap (0.36 V) than that of $Y@C_{2v}(9)\text{-}C_{82}$ (0.44 V), consistent with their different stabilities.[29]

Table 1: Redox potentials (V, versus Fc/Fc^+) of $Y@C_s(6)\text{-}C_{82}$[a] and $Y@C_{2v}(9)\text{-}C_{82}$.[b]

Compound	$^{ox}E_1$ [V]	$^{red}E_1$ [V]	$^{red}E_2$ [V]	$^{red}E_3$ [V]
$Y@C_s(6)\text{-}C_{82}$	−0.07	−0.43	−1.43[c]	−2.05
$Y@C_{2v}(9)\text{-}C_{82}$	+0.10	−0.34	−1.34[c]	−2.22

[a] Determined by differential pulse voltammetry in 1,2-dichlorobenzene with 0.1 M $(n\text{-}Bu)_4NPF_6$ at a Pt working electrode. [b] Data from Ref. [13]. [c] Two-electron process.

In summary, the long-sought labile $Y@C_{82}$ isomer has been isolated and characterized for the first time. Its cage structure and the metal position are firmly established by single-crystal X-ray diffraction, representing the first crystallographic identification of trivalent $M@C_s(6)\text{-}C_{82}$. Interestingly, an unprecedented dimerization occurs for $Y@C_s(6)\text{-}C_{82}$, which is the first reported dimeric structure of pristine EMFs in the crystalline state. In contrast, $Y@C_{2v}(9)\text{-}C_{82}$ does not form dimers under identical crystallization conditions. DFT calculations reveal that a special carbon atom on the cage of $Y@C_s(6)\text{-}C_{82}$ accumulates rather high spin density as a consequence of cage symmetry and metal location which leads to the regioselective dimerization of $Y@C_s(6)\text{-}C_{82}$ in the crystalline state. In contrast, the spin density is more evenly distributed on the cage of $Y@C_{2v}(9)\text{-}C_{82}$, most probably due to the moving metal atom, in addition to the cage symmetry. Moreover, the two $Y@C_{82}$ isomers also show different electronic structures and electrochemical properties as a consequence of different cage symmetry. The successful isolation of this labile $Y@C_{82}$ isomer has not only solved the long-lasting puzzle of its molecular structure and metal position (and presumably also confirms the molecular structures of

$La@C_{82}\text{-}II$ and $Pr@C_{82}\text{-}II$), but may also stimulate further interest in the exploration of such labile endohedral fullerenes, which may show fascinating chemical properties and potential spintronics applications.

[1] A. Popov, S. Yang, L. Dunsch, *Chem. Rev.* **2013**, *113*, 5989–6113.
[2] X. Lu, L. Echegoyen, A. L. Balch, S. Nagase, T. Akasaka, *Endohedral Metallofullerenes: Basics and Applications*, CRC, Boca Raton, **2014**.
[3] Y. Chai, T. Guo, C. M. Jin, R. E. Haufler, L. P. F. Chibante, J. Fure, L. H. Wang, J. M. Alford, R. E. Smalley, *J. Phys. Chem.* **1991**, *95*, 7564–7568.
[4] K. Kobayashi, S. Nagase, *Chem. Phys. Lett.* **1998**, *282*, 325–329.
[5] T. Akasaka, T. Wakahara, S. Nagase, K. Kobayashi, M. Waelchli, K. Yamamoto, M. Kondo, S. Shirakura, S. Okubo, Y. Maeda et al., *J. Am. Chem. Soc.* **2000**, *122*, 9316–9317.
[6] T. Akasaka, T. Wakahara, S. Nagase, K. Kobayashi, M. Waelchli, K. Yamamoto, M. Kondo, S. Shirakura, Y. Maeda, T. Kato et al., *J. Phys. Chem. B* **2001**, *105*, 2971–2974.
[7] T. Akasaka, X. Lu, H. Kuga, H. Nikawa, N. Mizorogi, Z. Slanina, T. Tsuchiya, K. Yoza, S. Nagase, *Angew. Chem. Int. Ed.* **2010**, *49*, 9715–9719; *Angew. Chem.* **2010**, *122*, 9909–9913.
[8] M. Takata, B. Umeda, E. Nishibori, M. Sakata, Y. Saitot, M. Ohno, H. Shinohara, *Nature* **1995**, *377*, 46–49.
[9] M. Hoinkis, C. S. Yannoni, D. S. Bethune, J. R. Salem, R. D. Johnson, M. S. Crowder, M. S. Devries, *Chem. Phys. Lett.* **1992**, *198*, 461–465.
[10] H. Shinohara, H. Sato, Y. Saito, M. Ohkohchi, Y. Ando, *J. Phys. Chem.* **1992**, *96*, 3571–3573.
[11] S. Suzuki, S. Kawata, H. Shiromaru, K. Yamauchi, K. Kikuchi, T. Kato, Y. Achiba, *J. Phys. Chem.* **1992**, *96*, 7159–7161.
[12] J. H. Weaver, Y. Chai, G. H. Kroll, C. Jin, T. R. Ohno, R. E. Haufler, T. Guo, J. M. Alford, J. Conceicao, L. P. F. Chibante et al., *Chem. Phys. Lett.* **1992**, *190*, 460–464.
[13] K. Kikuchi, Y. Nakao, S. Suzuki, Y. Achiba, T. Suzuki, Y. Maruyama, *J. Am. Chem. Soc.* **1994**, *116*, 9367–9368.
[14] L. Feng, T. Wakahara, T. Tsuchiya, Y. Maeda, Y. F. Lian, T. Akasaka, N. Mizorogi, K. Kobayashi, S. Nagase, K. M. Kadish, *Chem. Phys. Lett.* **2005**, *405*, 274–277.
[15] X. Lu, H. Nikawa, L. Feng, T. Tsuchiya, Y. Maeda, T. Akasaka, N. Mizorogi, Z. Slanina, S. Nagase, *J. Am. Chem. Soc.* **2009**, *131*, 12066–12067.
[16] W. Krätschmer, L. D. Lamb, K. Fostiropoulos, D. R. Huffman, *Nature* **1990**, *347*, 354–358.
[17] T. Akasaka, S. Okubo, M. Kondo, Y. Maeda, T. Wakahara, T. Kato, T. Suzuki, K. Yamamoto, K. Kobayashi, S. Nagase, *Chem. Phys. Lett.* **2000**, *319*, 153–156.

[18] Crystal Data for [Y@C_s(6)-C_{82}]$_2$·2[Ni(OEP)]·3(C_6H_6)·2(CS_2): black blocks, $0.06 \times 0.03 \times 0.02$ mm, monoclinic, space group $C2/m$, $a = 26.3952(12)$ Å, $b = 17.0335(8)$ Å, $c = 17.9502(8)$ Å, $\beta = 108.127(2)°$, $V = 7669.9(6)$ Å^3, $Fw = 3716.96$, $\lambda = 0.71073$ Å, $Z = 2$, $D_{calc} = 1.609$ Mg m^{-3}, $\mu = 1.122$ mm^{-1}, $T = 173$ K; 55016 reflections, 7374 unique reflections; 5275 with $I > 2\sigma(I)$; $R1 = 0.0753$ [$I > 2\sigma(I)$], $wR2 = 0.2373$ (all data), GOF (on F^2) $= 1.027$. The maximum residual electron density is 1.485 e Å^{-3}. Crystallographic data has been deposited in the Cambridge Crystallographic Data Center (CCDC 1470349), which contain the supplementary crystallographic data for this paper. These data can be obtained free of charge from The Cambridge Crystallographic Data Centre via www.ccdc.cam.ac.uk/data_request/cif.

[19] Crystal Data for 2[Y@C_{2v}(9)-C_{82}·2[Ni(OEP)]·3(C_6H_6)·2(CS_2): black block, $0.04 \times 0.04 \times 0.02$ mm, monoclinic, space group $C2/m$, $a = 26.6959(13)$ Å, $b = 17.2014(9)$ Å, $c = 17.8347(9)$ Å, $\beta = 107.0750(10)°$, $V = 7828.8(7)$ Å^3, $Fw = 3716.96$, $\lambda = 0.71073$ Å, $Z = 2$, $D_{calc} = 1.577$ Mg m^{-3}, $\mu = 1.099$ mm^{-1}, $T = 173$ K; 56593 reflections, 7463 unique reflections; 4796 with $I > 2\sigma(I)$; $R1 = 0.1248$ [$I > 2\sigma(I)$], $wR2 = 0.3765$ (all data), GOF (on F^2) $= 1.077$. The maximum residual electron density is 1.139 e Å^{-3}. Crystallographic data has been deposited in the Cambridge Crystallographic Data Center (CCDC 1470352), which contains the supplementary crystallographic data for this paper..

[20] M. Suzuki, Z. Slanina, N. Mizorogi, X. Lu, S. Nagase, M. M. Olmstead, A. L. Balch, T. Akasaka, *J. Am. Chem. Soc.* **2012**, *134*, 18772 – 18778.

[21] H. Yang, H. X. Jin, X. Q. Wang, Z. Y. Liu, M. L. Yu, F. K. Zhao, B. Q. Mercado, M. M. Olmstead, A. L. Balch, *J. Am. Chem. Soc.* **2012**, *134*, 14127 – 14136.

[22] Y. Maeda, S. Sato, K. Inada, H. Nikawa, M. Yamada, N. Mizorogi, T. Hasegawa, T. Tsuchiya, T. Akasaka, T. Kato et al., *Chem. Eur. J.* **2010**, *16*, 2193 – 2197.

[23] L. Feng, T. Tsuchiya, T. Wakahara, T. Nakahodo, Q. Piao, Y. Maeda, T. Akasaka, T. Kato, K. Yoza, E. Horn et al., *J. Am. Chem. Soc.* **2006**, *128*, 5990 – 5991.

[24] M. Yamada, H. Kurihara, M. Suzuki, M. Saito, Z. Slanina, F. Uhlik, T. Aizawa, T. Kato, M. M. Olmstead, A. L. Balch et al., *J. Am. Chem. Soc.* **2015**, *137*, 232 – 238.

[25] T. Wakahara, H. Nikawa, T. Kikuchi, T. Nakahodo, G. M. A. Rahman, T. Tsuchiya, Y. Maeda, T. Akasaka, K. Yoza, E. Horn et al., *J. Am. Chem. Soc.* **2006**, *128*, 14228 – 14229.

[26] H. Nikawa, T. Kikuchi, T. Wakahara, T. Nakahodo, T. Tsuchiya, G. M. A. Rahman, T. Akasaka, Y. Maeda, K. Yoza, E. Horn et al., *J. Am. Chem. Soc.* **2005**, *127*, 9684 – 9685.

[27] X. Lu, H. Nikawa, K. Kikuchi, N. Mizorogi, Z. Slanina, T. Tsuchiya, T. Akasaka, S. Nagase, *Angew. Chem. Int. Ed.* **2011**, *50*, 6356 – 6359; *Angew. Chem.* **2011**, *123*, 6480 – 6483.

[28] H. Nikawa, T. Yamada, B. P. Cao, N. Mizorogi, Z. Slanina, T. Tsuchiya, T. Akasaka, K. Yoza, S. Nagase, *J. Am. Chem. Soc.* **2009**, *131*, 10950 – 10954.

[29] M. D. Diener, J. M. Alford, *Nature* **1998**, *393*, 668 – 671.